UDK: 678.675:620.193.91
COSATI: 11-04, 19-04

Analysis of Smart Aramid Fiber Reinforced Laminar Thermoplastic Composite Material Under Static Loading

Irena Živković, PhD (Eng)[1)]
Katarina Maksimović, MSc (Eng)[2)]
Aleksandar Kojović, PhD (Eng)[3)]
Radoslav Aleksić, PhD (Eng)[3)]

In order to obtain a composite material with desired improved resistance to penetration of ballistic projectiles, a poly(p-phenyleneterephthalamide) reinforced laminar thermoplastic composite material has been made. This paper describes the procedure of manufacturing such a composite material, as well as the procedure of embedding fiber-optic sensors (FOS) in it, using the hot-melt method. Optical fibers were embedded in specimens of composite materials as intensity-based real-time damage detection sensors. Manufactured composite specimens with embedded FOS were subjected to static loading indentation. The initiation of damage and fracture during testing was detected by observation of the characteristic changing of the optical signal. The results of the experiments confirmed that optical fibers might be applied as intensity sensors in real-time monitoring of structural changes in thermoplastic laminate composite materials. The finite element method (FEM) modeling was used to analyze stress and displacement distributions through the layered composite plate, caused by indentation, and to simulate the contact problem - projectile/composite plate. The finite element simulation results of the considered layered composite plate have shown very good agreement with the experimental results.

Key words: **composite materials, thermoplastic materials, laminar materials, smart materials, ballistic protection, optical fiber, stress analysis, FEM.**

Introduction

PARA-ARMID fabrics are known for their remarkable performance, especially good thermic resistance, high tensile strength and toughness [1÷4]. Combining those fiber characteristics with thermoset matrix properties results in excellent composite reinforcing capabilities and hence improved ballistic protection [5÷9].

In addition to classical methods for damage detection in composite materials with polymer matrix (ultrasound [10], acoustic emission [11,12]), fiber-optic sensors (FOS) are widely used to monitor and precisely estimate material behavior during its manufacturing and exploitation life. Different FOS configuration can be found which mostly depends on optical fiber types being used and their light sensitivity. Numerous investigations on Smart Materials with embedded interferometric FOS such as Fabry-Perot [13-15], Michelson [16], and Bragg grating sensors [17-21] were made.

The shape and structure of intensity based optical fiber sensors allow their simple embedding in the host material without disturbing its basic mechanical properties, and therefore, they can be used as reliable, long-term automated sensors for real time structure damage and deformation detection [22,23]. Many authors noticed delamination within composite structures by using intensity-based FOS [24-27] and studied damage detection caused by low energy impact [28,29]. Hofer [30] has embedded a net of uncoated FOS of different diameters into the GFRP (Glass Fiber Reinforced Plastic) and CFRP (Carbon Fiber Reinforced Plastic). Purpose of his investigation was a possibility of exploitation of such smart material as a component in an Airbus production line. During his study, he managed to develop a system for automated indication of the damage that is invisible by bare eye, but detectable from the pilot cabin in real time. This system has opened a possibility for routine control minimization or even its abrogation.

Most of investigated composites contain thermoreactive polymer as a matrix. Preliminary investigation made on the-rmoplastic composite material aramid fiber/poly (vinylbutyral) [31] has shown that this specific material has the energy absorption capacity 5.5 higher than the same capacity of traditionally used materials with the same reinforcement, but mechanisms of its energy absorption had not been adequately explained, which is a subject of investigation in this article. Intensity-based FOS were embedded in referred material and completely smart material was tested by indentation. The finite element method (FEM) was used to analyze stress and displacement distributions through the layered composite plate, caused by indentation, and to simulate the contact problem - projectile/composite plate. Detailed finite element descriptions of numerical simulation behavior of smart aramid fiber reinforced composite material under static loading are given in references [33-37].

[1)] Institurte of Security, Kraljice Ane bb, 11000 Belgrade, SERBIA
[2)] City of Belgrade-City Government, Secretariat for Comunal and Housing Affairs Office of Water managment, Belgrade, SERBIA
[3)] Faculty of Technology and Metallurgy, Karngijeva 4, 11000, Belgrade, SERBIA

Properties of Material Components

Properties of reinforcement

Kevlar 129 fibers in a form of woven fabric, of a superficial mass of 280 g/m^2, were used as composite reinforcing material. The properties of Kevlar 129 are shown in Table 1.

Table 1. Properties of aramid fibers[1]

Density, g/cm^3	1.44
Ultimate tensile strength, cN/tex	235
Tensile strength, MPa	3380
Elongation at break point, %	3.4
Moisture content, %	7
Decomposition temperature, °C	560
Sound velocity, m/s	8660

Matrix properties

Thin PVB foils were used as a matrix in composite material. The properties of thermoplastic
PVB are shown in Table 2.

Table 2. Thermoplastic matrix properties[2]

Density, g/cm^3	1.058
Refractive index	1.48
Tensile strength, MPa	23
Elongation at break, %	210
Tensile modulus, MPa	5
Poisson's ratio	±0.5
Shore "A" Hardness	64
Specific heat, J/kgK	2100
Glass transition temperature, °C	16
Thermal conductivity, W/mK	0.21
Dielectric constant at 1 kHz	4
Dissipation factor at 1 kHz	1.8 10-4

Description of Composite Shaping Process

Composite specimens were made by uniform lamination of Kevlar fabric layers and PVB foils and then hot-pressed in a Teflon coated mold. Afterwards, specimens were left in a mold under slightly increased working pressure to cool from the maximal working temperature of 190°C to 100°C, and then were taken out of the mold to cool at room temperature under a load of 10 kg [31]. The parameters of the optimal working regime are shown in Fig.1. At the end, total masses of specimens were measured and the mass percentage of specimen's specific components was calculated. The results are listed in Table 3.

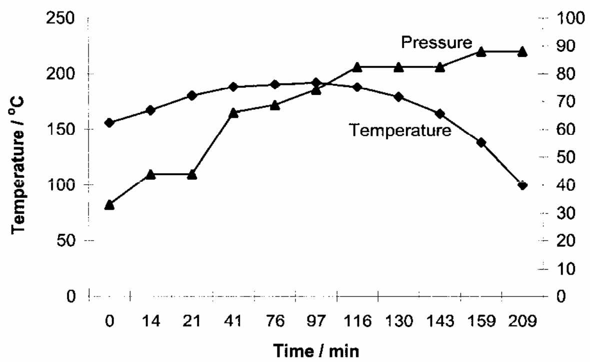

Figure 1. Optimal regime of laminated composite material hot-pressing

[1] Original properties given by manufacturer

Table 3. Specimens total mass, mass percentage of specific components

Specimen	Type of reinforcement	Reinforce-ment mass, g	Total specimen mass, g	Mass % of reinforce-ment	Mass % of ma-trix
O2	Aramid fabric	150,0	230,0	65,2	34,8

Optical Fibres Embedding Procedure

Three optical fibres were embedded in the produced composite specimen O2. The fibers were placed in parallel to the specimen surface and covered with additional layers of the matrix and the reinforcement. The specimens were hot-pressed again with simultaneous real-time monitoring of the light signal intensity drop. The diagram of the light signal intensity drop during the embedding of the optical fibers into the composite material (Fig.2) clearly shows that there was no permanent drop or complete loss of signal detected, which indicates that the fibers did not suffer significant damage during the embedding process. The photo of the specimen after the described embedding process is shown in Fig.3.

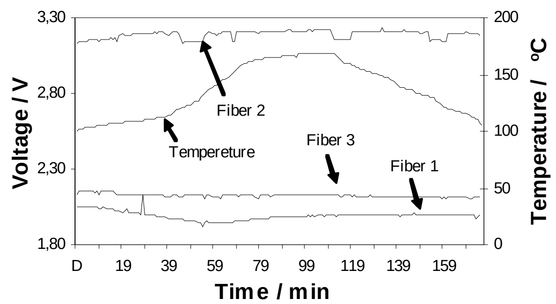

Figure 2. Light signal intensity drop measurement during the optical fibers embedding into the composite material

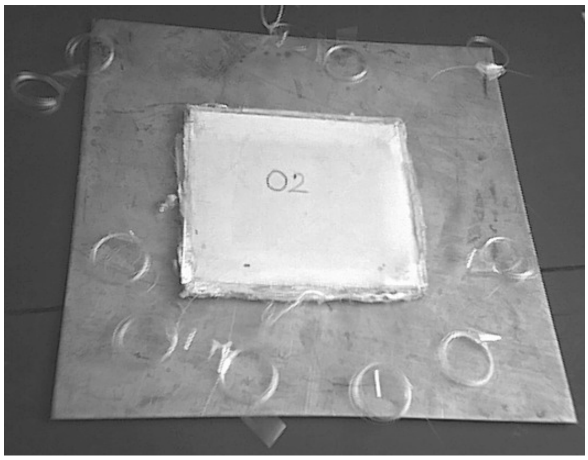

Figure 3. Photo of the composite material specimen with the embedded optical fibers

The optical fiber sensors were embedded into the last layer of the composite material according to the previously described procedure [32].

The mechanical properties of the manufactured laminar composite material are listed in Table 4.

Table 4. Mechanical properties of the composite material aramid fabric/ PVB matrix

E_{11}, GPa	E_{22}, GPa	E_{33}, GPa	G_{12}, GPa	G_{13}, GPa	G_{23}, GPa	ν_{12}	ν_{13}	ν_{23}	Density ρ, kg/m^3
149.9	149.8	3	4	4	4	0.3	0.2	0.2	1413

Test results and the discussion of the static load effect on the composite material

Testing by means of embedded fiber optic sensors

The manufactured composite specimens with optical fibers were subjected to static loading by the adapted tensile testing machine. The specimens were tested in a case when the loading was directed onto the bottom layer (the furthest po-sition of the optical fibers from the indentation loading point).

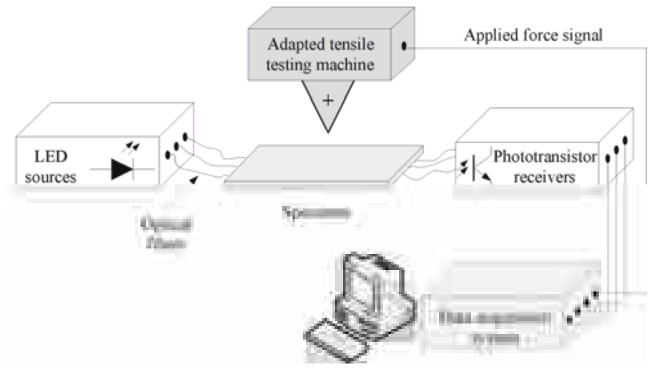

Figure 4. Measuring and acquisition part of the equipment

The opto-electronic part of the measurement system consists of three emitter diodes as a light source for optical fibers, and three photo detectors for light intensity measurement. It is shown in Fig.4. The load was permanently measured during testing by the load measurement converter. The acquisition of the output signals from the photodetectors and the load converter was conducted using the AD converter card and a personal computer. The acquisition software, written in Pascal, provides simultaneous 16-channel signal sampling as well as changing of the sampling rate, so the load and the photodetector output signals were monitored simultaneously for all three fibers embedded in one specimen. The indentator position is shown in Fig.5.

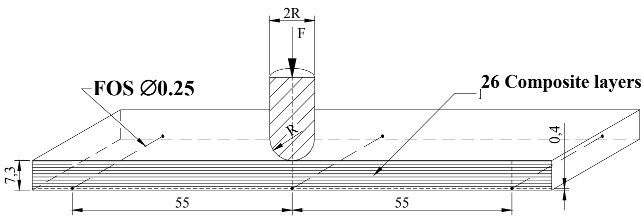

Figure 5. Position of the indentator during testing

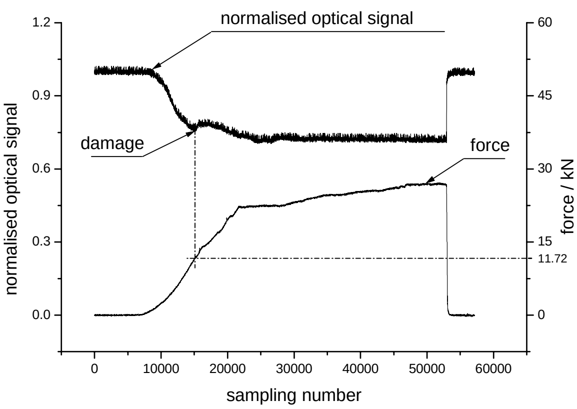

Figure 6. Signal intensity changes during indentation

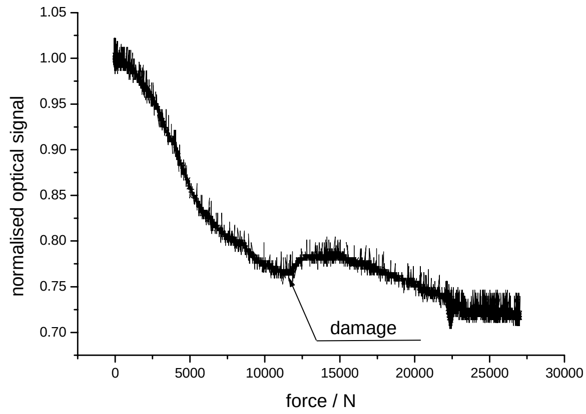

Figure 7. Signal intensity changes in a function of the applied force

The graphs presented in Fig.5 show the time dependence of the normalized light intensity signal through the optical fiber placed exactly under the indentation point, as well as the applied load during the indentation testing. In Fig.6 the normalized optical signal intensity versus the applied load is presented. From Figures 6 and 7 it could be seen that the light intensity drop is proportional to the load until the first local minimum in a normalized optical signal (denoted as damage in Figures 6. and 7) has happened. Hence, at a force value of 11.72 kN the signal intensity increases which indicates the local stress decrease. The explanation of this phenomenon can be the fact that the indentator, after piercing through the first layer of the composite plate, ran into the layer of the thermoplastic matrix. This is a medium of lower strength than the composite one and therefore the area of lesser local stress around the optical fiber. The signal intensity increases until the point when the indentator touches the second layer of the composite material, renewing stress around the fiber and decreasing the signal intensity as a consequence. The applied force causes microbending of the optical fiber and changing of the shape cross-section. After unloading, the signal intensity restores its initial value, which indicates the undamaged structure of optical fibers during tests. The maximum value of the applied force was 27.50 kN.

Indentator displacement disposition

Specimen indentation was performed with the compression strength testing machine. As an indentator, an 11.287 mm diameter steel ball was used. The ball was blackened before indentation in order to obtain a clear indentation mark. The indentation mark diameters were measured by the micrometer, and the mark depth (w) and the compression strength (HB) were calculated. The test results are listed in Table 3.

The functional relationship between the indentator displacement and the applied force is shown in Fig.8. The microscope photos for corresponding points are shown below the picture – the point D where there is no detected initial damage of the first layer within the material, the point E where initial reinforcement failure occurs and changes the curve slope, and finally, the point H, which is the final point of testing.

Table 5. Experimental and calculated results of the compression strength determination

Point	Load, kg	Mark diame-ter d, mm	Mark depth w, mm	Force F, daN	Compression strength HB, MPa
A	800	4.750	0,52	784.8	422.6
I	860	4.790	0.53	843.7	446.4

B	900	4.850	0.55	882.9	455.0
C	1000	5.060	0.60	981.1	462.3
D	110	5.280	0.66	1079.1	464.5
G	1150	5.330	0.67	1128.1	476.0
E	1200	5.430	0.70	1177.2	477.3
F	1250	5.950	0.85	1226.2	408.1
H	1320	6.552	1.05	1294.9	348.6

The obtained results show sudden change of the curve slope after the point E where the applied force is 11.772 kN. This slope change indicates that the first layer failure happens at the mentioned value of the applied force. Sudden increase of the indentator displacement values is also a consequence of the assumed first layer failure within the composite material reinforcement and decrease of the material resistance for a specific value of the applied force.

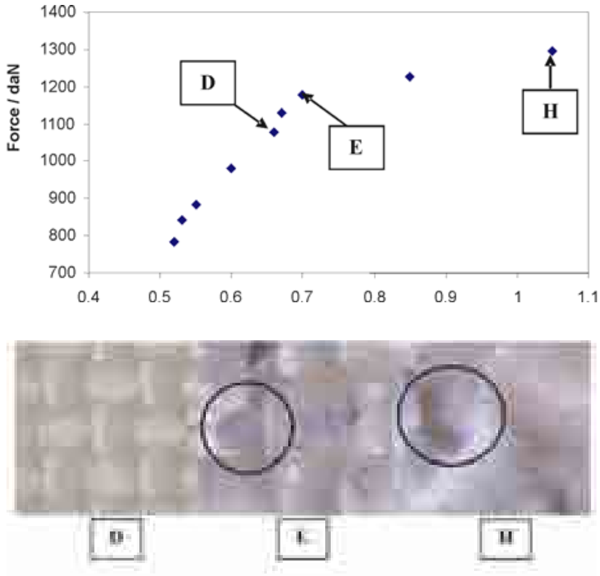

Figure 8. Functional relationships between the indentator displacements and the applied force along with the microscope photos of the characteristic indentation points

The composite plate contact stress analysis by the Finite Element Method

The Finite Element Method (FEM) can be successfully used for the static and dynamic stress analysis [33-37]. In the present study, we investigated the stress distributions at the laminated plate under static load introduced by the steel indentator. For this purpose a three-dimensional finite element method was applied to calculate stress distributions at the laminated composite plate. The analysis was performed on the 15 deg circular segment of the composite plate, 18.5 mm in length and 7.3 mm in thickness, placed on a horizontal rigid surface, with a hemispherical hardened steel indentator of 11.287 mm in diameter. A circular segment of 15 degrees for the FE analysis of the composite plate was used for the simplicity reason. A 7.3 mm thick composite plate was made of 26 layers of aramid fabric as reinforcement and PVB matrix. The plate was modeled with 3D solid finite elements. The mechanical properties for such 3D elements are those defined - measured for the composite specimen (Table 4). The mechanical properties of the indentator material are listed in Table 6. The specimen was cut out from the analyzed composite plate. The geometric nonlinear static FE analysis in the contact region was done by using the 'slide line' type finite elements. The Finite Element Analysis is carried out using the MSC/NASTRAN code, which is characterized by advanced capabilities for a structural contact analysis.

Table 6. Mechanical properties of the indentator material

Modulus of Elasticity E, GPa	Shear Modulus G, MPa	Poisson`s ratio ν	Density ρ, kg/m^3
500	193.8	0.29	7820

The results obtained in the experiment – measured displacement/penetration of the indentator in the composite plate *vs.* applied force and the calculated compression strength HB are given in Table 5.

For a set of the applied compression force F, daN, a corresponding mark of the penetrating depth 'w', mm in the composite plate is measured.

The stress and displacement distribution in the finite element model of the composite plate segment are shown in Figures 9, 11 and 12 for the case of compression force F=11.772 kN, w=0.7 mm.

Table 7. Displacement-compression force relationship obtained by the experiment and the FEM

Point	Compression force F (daN)	Displacement-experiment (mm)	Displacement-FEM (mm)
A	784.8	0.52	0.528
I	843.7	0.53	0.554
B	882.9	0.55	0.572
C	981.1	0.60	0.613
D	1079.1	0.66	0.654
G	1128.1	0.67	0.672
E	1177.2	0.70	0.691
F	1226.2	0.85	0.710
H	1294.9	1.05	0.738

There is quite a good agreement between the simulated results and the experimental ones, 1-3 % in the region before the point E. For further force increase, the FE analysis in this case, makes no sense because the first reinforcement layer has failed. As it can be seen, this FE analysis method for this composite plate is quite adequate.

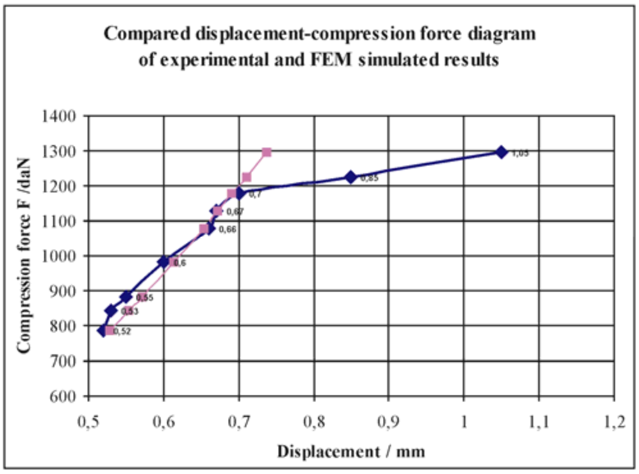

Figure 9. FEM- Experiment displacement vs. compression force results

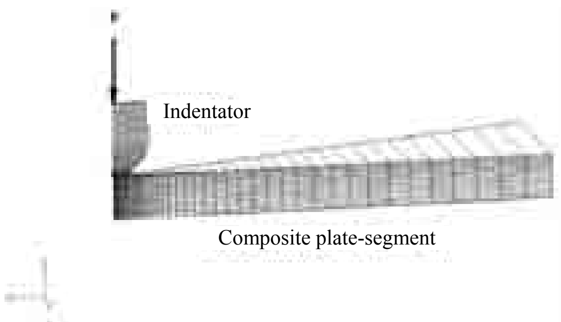

Figure 10. FEM model of the composite segment

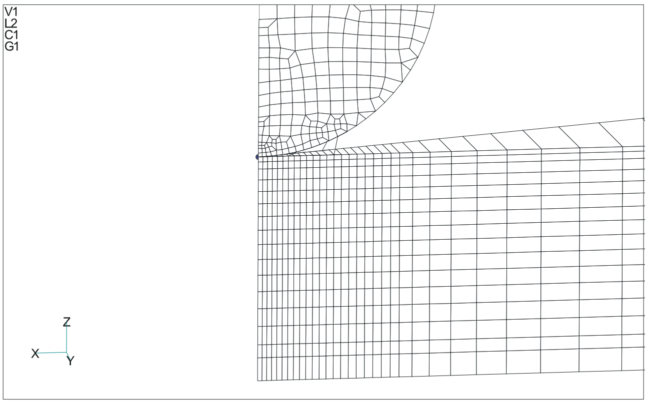

Figure 11. Mesh of finite elements in the contact zone, magnified

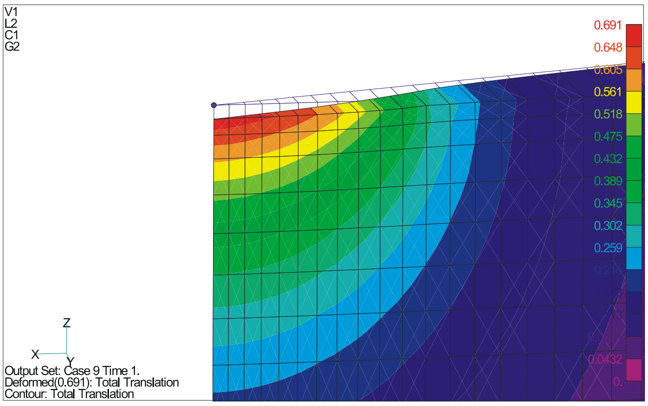

Figure 12. Distribution of displacement, mm in contact zone - indentation mark depth, magnified

The force *vs*. displacement experimental and FE analysis results are listed in Table 5 and Fig.9. The diagram shows a characteristic point E (compression force F=11.772 kN, *w*=0.7 mm; *F* =0.49 kN for segment) at which the first layer failure occurred. A relatively small increase of the applied force causes a large increase in displacement – depth '*w*' (points F and H).

Conclusion

In the processing of poly (p-phenyleneterephthalamide) reinforced laminar thermoplastic composite material, optimal shaping parameters were obtained, as well as optimal resin content.

The subject of the experiment was the analysis of aramid fibers-PVB ballistic composite materials with embedded optical fibers as intensity sensors for detection of real-time mechanical damage and deformations. The light signal intensity drop is an optical fiber response to the applied static loading on composite material. The main goal of experiment is to develop a system for thermoplastic composite structure health monitoring during composite processing and real life exploitation.

The experiments showed that the signal intensity drop through optical fibers occurs when stress through material is carried over onto them. An embedded set of optical fibers is an efficient way to estimate what is happening within thermoplastic composite material when it is subjected to static loading.

The testing results showed that failure of the first reinforcement layer occurs at 11.77 kN of the applied force. At this point, the indentator displacement was 0.7 mm, which is also described as a peak value in the signal intensity-applied force diagram. A good agreement between the model made by the finite element analysis and the experiment was obtained.

The results presented in this paper confirm a possibility to apply optical fibers as intensity sensors for health monitoring of thermoplastic laminate aramid-PVB composite materials, under real-time conditions of static loading.

References

[1] TOHLEN,M.E.: Generation of Design Allowables, Engineered Materials Handbook ASM; 1998, Vol.1, pp.308-312.

[2] WARDLE,M.W.: Designing Composite Structure for Toughness, Technical Symposium V, Design and Use of Kevlar Aramid Fiber in Composite Structures, 1984

[3] JONES,F.R.: Handbook of Polymer-Fiber Composites, Longman, 29-48, 231-234, 265-285, 1994

[4] CLYNE,T.W., JONES,F.R.: Composites: Interfaces, Encyclopedia of Materials: Science & Technology, Part Composites, Elsevier; 2001

[5] KASANO: Recent advances in high-velocity impact perforation of fiber composite laminates [Review], JSME International Journal Series A-Solid Mechanics & Material Engineering. 42(2),147-157, 1999 Apr.

[6] CHEN,J.K., MEDINA,D.F.: The effects of projectile shape on laminated composite perforation, Composites Science & Technology.58(10), 1629-1639,1998.

[7] WEN,H.M., REDDY,T.Y., REID,S.R., SODEN,P.D.: Indentation, penetration and perforation of composite laminates and sandwich panels under quasi-static and projectile loading, Book Editors Kim JK, Yu TX, Impact Response and Dynamic Failure of Composites and Laminate Materials, pts 1 and 2. 141-1(Part 1-2) PG. 501-552. 1998 [Figures] [Plates].

[8] ZEE,R.H., HSIEH,C.Y.: Energy absorption processes in fibrous composites, Materials Science & Engineering A-Structural Materials Properties Microstructure & Processing. 246(1-2),161-168, 1998 May 15.

[9] GELLERT,E.P., PATTIE,S.D., WOODWARD,R.L.: Energy transfer in ballistic perforation of fiber reinforced composites, Journal of Materials Science. 33(7), 1845-1850, 1998 Apr.

[10] POTEL,C., CHOTARD,T., BELLEVAL,J.F., BENZEGGAGH,M.: Characterization of composite materials by ultrasonic methods: modelization and application to impact damage, Composites B 29B (1998), pp.159-169.

[11] HASELBACH,W., LAUKE,B.: Acoustic emission of debonding between fibre and matrix to evaluate local adhesion, Comp. Sci. Teh. 63 (2003), pp. 2155-2162.

[12] SUNG,D., KIM,C., HONG,C.: Monitoring of impact damages in composite laminates using wavelet transform, Composites B 33 (2002), pp. 35-43.

[13] BOGDANOVICH,A.E., WIGENT III D.E., WHITNEY,T.J.: Fabrication of 3-D woven preforms and composites with integrated fiber optic sensors, SAMPE Journal 39 4 (2003), pp. 6-15.

[14] KALAMKAROV,A., FITZGERALD,S., MACDONALD,D. GEORGIADES,A: The mechanical performance of composite rods with embedded fiber-optic sensors, Comp Sci Tech 60 (2000), pp. 1161-1169.

[15] MALKI,A., GAFSI,R., MICHEL,L., LABARRERE M., LECOY,P.: Impact and vibration detection in composite materials by using intermodal interference in multimode optical fibers, Applied Optics 35 25 (1998), pp. 5198-5201.

[16] KWON,I.B., KIM,C.G., HONG,C.S.: Simultaneous sensing of the strain and points of failure in composite beams with an embedded fiber optic Michelson sensor, Comp Sci Tehn 57 (1997), pp. 1639-1651.

[17] KUANG,K.S.C., KENNY,R., WHELAN,M.P., CANTWELL,W.J., CHALKER,P.R.: Embedded fibre Bragg grating sensors in advanced composite materials, Comp. Sci. Tech. 61 (2001), pp. 1379-1387.

[18] JONES,R., GALEA,S.: Health monitoring of composite repairs and joints using optical fibres, Composite Structures 58 (2002), pp. 397-403.

[19] STUDER,M., PETERS,K., BOTSIS,J.: Method for determination of crack bridging parameters using long optical fiber Bragg grating sensors, Composites B 34 (2003), pp. 347-359.

[20] TAKEDA,S., OKAB,Y., TAKEDA,N.: Delamination detection in

CFRP laminates with embedded small-diameter fiber Bragg grating sensors, Composites A 33 (2002), pp. 971-980.

[21] PARK,J., LEE,S., KWON,O., CHOI,H., LEE,J.: *Comparison of nondestructive microfailure evaluation of fiber-optic Bragg grating and acoustic emission piezoelectric sensors using fragmentation test*, Composites A 34 (2003), pp. 203-216.

[22] HADŽIĆ,R., JOHN,S., HERSZBERG,I.: *Structural integrity analysis of embedded optical fibers in composite structures,* Composite Structures 47 (1999), pp. 759-765.

[23] SEO,D.C., LEE,J.J.: *Effect of embedded optical sensors on transverse crack spacing of SMART composite structures*, Composite Structures 32 (1995), pp. 51-58.

[24] RIPPERT,L., WEVERS,M., HUFFEL,S.: *Optical and acoustic damage detection in laminated CFRP composite materials,* Composite Science and Technology 60 (2000), pp. 2713-2724.

[25] USKOKOVIC,P.S., BALAC,I., BRAJOVIC,LJ., SIMIC,M., PUTIC,S. ALEKSIC,R.: *Delamination detection in woven composite laminates with enbedded optical fibers*, Advanced Engineering Materials 3 7 (2001), pp. 492-496.

[26] TAKEDA,N.: *Characterization of microscopic damage in composite laminates and real-time monitoring by embedded optical fiber sensors*, Int. J. of Fatigue 24 (2002), pp. 281-289.

[27] MEASURES,R.M., GLOSSOP,D.W., LYMER,J., LEBLANC,M., WEST,J., DUBOIS,S., TSAW,W., TENNYSON,R.C.: *Structurally integrated fiber optic damage assessment system for composite materials*, Applied Optics 28 13 (1989), pp. 2626-2633.

[28] KUANG,K.S.C.: CANTWELL,W.J.: *Detection of impact damage in thermoplastic-based fiber-metal laminates using optical fiber sensors*, J. of Mater. Sci. Lett. 21 (2002), pp. 1351-1354.

[29] USKOKOVIĆ,P.S., BRAJOVIC,LJ., SIMIC,M., PUTIC,S.S., AND ALEKSIC,R.: *An intensity based optical fiber sensor for low velocity impact detection in unidirectional composites,* Adv.Composite Mater. 9 3 (2000), pp. 175-185.

[30] HOFER,B.: *Fiber optic damage detection in composite structures*, Composites 18 4 (1987), pp. 309-316.

[31] ŽIVKOVIĆ,I., PERIŠIC,P., BURZIĆ,Z., USKOKOVIĆ,P., ALEKSIĆ,R.: *Aramid fiber reinforced laminar thermoplastic composite materials*, Proc. 23rd SAMPE Europe Int. Conf., Pariz, (2002), pp. 249-260.

[32] ŽIVKOVIĆ,I. BRAJOVIĆ,LJ., USKOKOVIĆ,P., ALEKSIĆ,R.: *Indentation damage detection in thermoplastic composite laminates by using embedded optical fibers*, Journal of Advanced Materials, in press (January 2006)

[33] MAKSIMOVIC,S., RUZIC,D., MAKSIMOVIC,K.: *An improved 4-node shell finite element used in postbuckling and failure analysis,* LUXFEM–1st International Conference on Finite Element for Process, Luxemburg, Luxemborg City, (2003), pp.13-14.

[34] MAKSIMOVIC,S.: *Improved geometrically nonlinear finite element analysis and failure fibre reinforced composite laminates,* Proc. of Fourth Int. Symp. on Brittle Matrix Composites, Warsaw, Poland, Woodhead Publ. Lim. Cambridge (1994).

[35] MAKSIMOVIC,S.: *Some Computational and Experimental Aspects of Optimal Design Process of Composite Structures*, Int. J. Composite Structures 17 (1990), pp 237-258.

[36] MAKSIMOVIC,S.: *Postbuckling and failure analysis of axially compressed composite panels using FEM*, Scientific Technical Review, 2007, Vol.LVII,No.3-4, pp.43-48.

[37] MAKSIMOVIC,S.: *FAILURE ANALYSIS OF LAYERED COMPOSITE STRUCTURES: Computation and Experimental Investigation,* ECF 16, 16th European Conference of Fracture, ECF 16, Alexandroupolis, Greece, 2006

[38] BAHEI-EL-DIN,Y.A, ZIRKY,M.A.: *Impact-induced deformation fields in 2D and 3D woven composites*, Composites Science and Technology 63 (2003), pp. 923-942.

Received: 05.02.2008.

Analiza SMART aramidnim vlaknom ojačanih laminarnih termoplastičnih kompozitnih materijala tokom statičkog opterećivanja: poređenje eksperimentalnih rezultata i numeričke simulacije

Sa ciljem dobijanja kompozitnog materijala poboljšane otpornosti na proboj balističkog projektila, napravljen je poli(p-fenilentereftalamidom) ojačan laminarni termoplastični kompozitni materijal. Ovaj rad opisuje postupak izrade ovog kompozitnog materijala, kao i postupak ugradnje fiber-optičkih senzora (FOS) u isti, upotrebom metode toplog presovanja. Optička vlakna su ugrađena u uzorke kompozitnih materijala kao intenzitetni senzori za detekciju oštećenja u realnom vremenu. Izrađeni kompozitni uzorci sa ugrađenim FOS su izlagani statičkom opterećenju utiskivanjem. Inicijalno oštečenje i lom tokom ispitivanja su detektovani padom inteziteta svetlosnog signala propuštenog kroz optička vlakna. Rezultati eksperimenata su potvrdili opravdanost upotrebe optičkih vlakana kao intenzitetnih senzora za praćenje strukturalnih promena u termoplastičnim laminarnim kompozitnim materijalima u realnom vremenu. Za analizu raspodele napona i deformacija po debljini višeslojne kompozitne ploče, pod dejstvom utiskivanja, korišćen je metod konačnih elemenata (MKE). Primenom MKE je simuliran kontaktni problem projektil/kompozitna ploča. Rezulatati MKE analize razmatrane kompozitne ploče su pokazali odlično slaganje sa eksperimentalnim rezultatima.

Ključne reči: **kompozitni materijali, termoplatični materijali, laminarni materijali, SMART materijali, balistička zastita, optičko vlakno, analiza napona, metoda konačnih elemenata.**

Анализ смарт-арамидовым волокном усиленных ламинарных термопластических композитных материалов в течении статической нагрузки

С целью получения композитного материала улучшеного сопротивления на пробивание баллистического снаряда, изготовлен поли (п-фенилентерефталамидом), усиленный ламинарный термопластический материал. Настоящая работа описывает поступок изготовления этого композитного материала, а в том числе и поступок встроения волокно-оптических (фибер-оптических) датчиков (FOS-fiber-optics sensors) в тот материал пользованием метода горячего плавления. Оптические волокна встроены в образцы композитных

материалов в роли интенсивных датчиков для обнаружения повреждений в реальном времени. Изготовленные композитные образцы со встроенными FOS подвергнуты статической нагрузке сжиманием. Начальное повреждение и излом в течении исследования обнаружены снижением интенсивности светового сигнала, пропущеного через оптические волокна. Результаты эксперимента потвердили обоснованность употребления оптических волокон в роли интенсивных датчиков для наблюдения изменений в структуре в термопластических ламинарных композитных материалах в реальном времени. Для анализа расспределения напряжений и деформаций по толщине многослойной композитной плиты, под действием сжимания, использован метод конечных элементов (МКЭ). Применением МКЭ симулированна контактная проблема снаряд/композитная плита. Результаты МКЭ анализа рассматриваемой композитной плиты показали отличное (полное) согласование с экспериментальными результатами.

Ключевие слова: **композитные материалы, термопластические материалы, ламинарные материалы, смарт-материалы, баллистическая защита, оптическое волокно, анализ напряжения, метод конечных элементов.**

Analyse des matériaux composites thermoplastiques laminaires renforcés par la fibre aramide smart durant la charge statique

En vue d'obtenir le matériau composite dont la résistance est améliorée quant à la pénétration du projectile balistique, on a fabriqué un matériau composite thermoplastique laminaire qui est renforcé par le poly (p-phényl–énétérephtalamide). Ce papier décrit le procédé de fabrication des senseurs fibre–optiques (SFO) par la méthode de la presse chauffante. Les fibres optiques sont incorporées dans les échantillons des matériaux comme les senseurs d'intensité pour la détection des dégâts dans le temps réel. Les échantillons composites fabriqués aux SFO incorporés ont été exposés à la charge statique par indentation. Le dégât initial et la fracture lors des essais ont été détectés par la diminution de l'intensité du signal lumineux à travers les fibres optiques. Les résultats des essais ont confirmé qu'il était possible d'utiliser les fibres optiques comme senseurs d'intensité pour la surveillance des changements structuraux chez les matériaux composites laminaires thermoplastiques dans le temps réel. Pour analyser la distribution de la tension et les déformations de l'épaisseur de la plaque composite à couches à plusieurs, causées par indentation, on a employé la méthode des éléments finis (MEF). En appliquant cette méthode on a simulé le problème du contact projectile/plaque composite. Les résultats de l'analyse MEF de la plaque composite considérée ont démontrés qu'il y avait très bon accord avec les résultats des essais.

Mots clés: **matériaux composites, matériaux thermoplastiques, matériaux laminaires, matériaux smart, protection balistique, fibre optique, analyse de tension, méthode des éléments finis.**